Charge and spin distributions in $Ga_{1-x}Mn_xAs/GaAs$ ferromagnetic multilayers

S. C. P. Rodrigues, L. M. R. Scolfaro, J. R. Leite,* and I. C. da Cunha Lima[†]
Instituto de Física, Universidade de São Paulo, CP 66318, 05315-970, São Paulo, SP, Brazil

G. M. Sipahi
Instituto de Física de São Carlos, Universidade de São Paulo, CP 369, 13560-970, São Carlos, SP, Brazil

M. A. Boselli[‡]
Instituto de Física, Universidade do Estado do Rio de Janeiro, Rua São Francisco Xavier 524, 20.500-013 Rio de Janeiro, R.J., Brazil
(Received 28 January 2004; revised manuscript received 25 May 2004; published 13 October 2004)

A self-consistent electronic structure calculation based on the Luttinger-Kohn model is performed on GaMnAs/GaAs multilayers. The diluted magnetic semiconductor layers are assumed to be metallic and ferromagnetic. The high Mn concentration (5% in our calculation) makes it possible to assume the density of magnetic moments as a continuous distribution, when treating the magnetic interaction between holes and the localized moments of the Mn^{++} sites. Within the supercell approach we calculated the distribution of heavy holes and light holes in the structure. We found a strong spin-polarization, the charge being concentrated mostly on the GaMnAs layers. This happens due to heavy and light holes with their total angular momentum antialigned to the average magnetization being attracted to these regions. The charge and spin distributions are analyzed in terms of their dependence on the number of multilayers, the widths of the GaMnAs and GaAs layers, and the width of the lateral GaAs layers at the borders of the structure.

DOI: 10.1103/PhysRevB.70.165308 PACS number(s): 73.21.−b, 75.75.+a, 85.75.−d, 72.25.Dc

I. INTRODUCTION

Recent advances in the physics and technology of GaAs-based nanostructures with diluted magnetic semiconductors (DMS) open up a wide range of potential applications of these systems in integrated magneto-optoelectronic devices.[1] In $Ga_{1-x}Mn_xAs$ alloys the substitutional Mn acts as an acceptor (it binds one hole), and at the same time carries a localized magnetic moment, due to its five electrons in the 3*d* shell. For x near 0.05, the alloy is a metallic ferromagnet,[2] the Curie-Weiss temperature after annealing is 160 K,[3] and the free hole concentration is near 10^{20-21} cm^{-3}. Potential relevance in spintronics and photonics applications arise because such a ferromagnetic layer can inject spin-polarized carriers into an otherwise nonmagnetic semiconductor region of the device, thus eliminating the need for a strong external magnetic field. The higher the transition temperature of a DMS layer, the higher the possibilities for a device to operate near room temperatures. Currently, the ferromagnetic order in the metallic phase is understood as resulting from the indirect exchange between the Mn^{2+} ions due to the local spin polarization of the hole gas. This explanation requires that the spin coherence length be larger than the average distance between the localized moments. Although most of the theoretical research on this problem has been directed towards understanding the origin of the ferromagnetism, there are still fundamental issues to be considered in the electronic structure. For instance, the role played by the light holes and holes of the split-off band in this DMS is an issue yet to be understood. Note that this nomenclature is specific for GaAs bulk systems, where the tetragonal symmetry is preserved. In the case of heterostructures, where such symmetry is broken by the presence of the interfaces, hole states are mixed. Differently from heavy holes, light hole states are not spin eigenstates. As a consequence, the occurrence of a local magnetic field due to the *sp-d* interaction is also a factor that contributes to the mixing in hole states. This can be easily seen in the framework of the effective mass approximation and Luttinger-Kohn (LK) $\mathbf{k}\cdot\mathbf{p}$ expansion,[4] because additional off-diagonal terms appear in the Hamiltonian, breaking the tetragonal symmetry. Therefore, the presence of interfaces, together with a local magnetic field, requires a proper calculation of the electronic properties in DMS heterostructures.

So far, the six-bands $\mathbf{k}\cdot\mathbf{p}$ method has been used to obtain the valence band structure of (Ga,Mn)As only in bulk systems,[5–8] except for Ref. 9 which calculated planar structures. Some calculations included the effects of biaxial strain, spin-orbit coupling, and exchange correlation in a parabolic band approximation.[10–12] In the case of quantum wells, (Ga,Mn)As multilayers and superlattices, a self-consistent calculation has been done for parabolic heavy holes subbands.[14] Self-consistent calculations have also been performed in Refs. 11 and 12 assuming isotropic effective masses. All of these electronic structure calculations assume a homogeneous density of magnetic moment, as well as homogeneous negative charge concentration due to the ionized Mn atoms. This is not the case of Ref. 13, where a Monte Carlo simulation is used. Relaxing this approximation implies a multiple-scattering treatment, which is beyond the scope of the present work. The homogeneous approximation for the density of magnetic and Coulomb scattering centers (localized magnetic moments and ionized impurities) provides important information concerning the carriers charge and spin distributions.

Here we present a self-consistent LK $\mathbf{k}\cdot\mathbf{p}$ calculation for GaMnAs/GaAs multilayers and superlattices. As described below, we carry out a supercell calculation which is an ex-

 ©2004 The American Physical Society

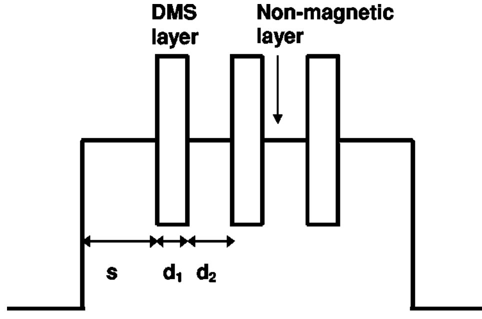

FIG. 1. The model structure: the DMS layers of width d_1 are separated by nonmagnetic GaAs layers of width d_2. At the left of the first DMS layer and at the right of the last one, GaAs lateral layers of width s complete the "active" parts. The "active" parts are separated, themselves, by thick AlAs barriers.

tension of the LK method to treat the cases of quantum wells and superlattices (SL). The structure we consider consists of substitutional Mn ions uniformly distributed in $Ga_{0.95}Mn_{0.05}As$ layers of width d_1, with a hole concentration of 1×10^{20} cm^{-3}. These layers are assumed to be metallic and ferromagnetic at $T=0$ K. The DMS regions are separated by nonmagnetic GaAs layers of width d_2. Adjacent to the first DMS layer and to the last one, GaAs lateral layers of width s cap the structure, as shown in Fig. 1. The supercell approach consists of placing this "active part," described so far, between thick layers of a large gap material, assumed here to be AlAs, and treating the whole system as a superlattice.

Our calculated spin and charge configurations provides information on the composition of heavy holes and light holes in the structure. Our carriers are heavy holes antiparallel to the DMS magnetization, and also antiparallel light holes, in a smaller amount. We found a strong spin polarization, the charge being concentrated mostly in the GaMnAs layers. In addition, we analyze the charge and spin distributions in terms of their dependence on the number of multilayers, the widths d_1 and d_2, as well as the widths of the lateral GaAs layers.

II. MAGNETIC INTERACTION IN THE CONFINED LK MODEL

The interaction between free holes and the localized magnetic moments is well described by the Kondo-type term,

$$V_{\mathrm{mag}}(\mathbf{r}) = -I\sum_i \vec{s}(\mathbf{r})\cdot\mathbf{S}(\mathbf{R}_i)\,\delta(\vec{r}-\mathbf{R}_i), \tag{1}$$

where I is the *sp-d* interaction. The localized spin of the Mn ion $\vec{S}_i$ at position $\vec{R}_i$ is treated as a classicalvariable, since it results of the five 3 d electrons obeying Hund's rule, and no hybridization with carriers is considered, due to the high difference in energies. $\vec{s}(\vec{r})$ is the spin operator of the carrier at position $\vec{r}$. At zero temperature, assuming a complete alignment of the localized magnetic moment, i.e., $\mathbf{S}(\mathbf{R}_i)=\mathbf{S}$, we have:

$$V_{\mathrm{mag}}(\vec{r}) = -I\mathbf{S}\cdot\vec{s}(\vec{r})\sum_i \delta(\vec{r}-\mathbf{R}_i) = -\frac{I}{2}\mathbf{S}\cdot\vec{\sigma}\rho_i(\vec{r}). \tag{2}$$

In the last expression we used $\vec{\sigma}=\hat{i}\sigma_x+\hat{j}\sigma_y+\hat{k}\sigma_z$ to denote the three Pauli matrices; $\rho_i(\vec{r})$ is the density of magnetic impurities. Assuming a homogeneous distribution of the localized magnetic dipoles inside the DMS layers, we have $\rho_i(\vec{r})\approx xN_0g(z)$, where N_0 is the density of cations, x is the substitutional concentration of Mn, and $g(z)=1$ if z lies inside a DMS layer, $g(z)=0$ otherwise. In that case the magnetic interaction becomes

$$V_{\mathrm{mag}}(z) = -\frac{x}{2}N_0\beta g(z)\vec{M}\cdot\vec{\sigma}. \tag{3}$$

In Eq. (3) we have explicitly taken into consideration that carriers are holes, replacing I by β. For GaMnAs, $N_0\beta=-1.2$ eV.[15] For electrons, $N_0\alpha=0.2$ eV.[16] Were the spin of the particles well defined, this term would represent, in bulk, a shift on the top (bottom) of the valence (conduction) band. This is not the case, as discussed above, for light holes and split-off holes in GaAs.

It is well known that the valence bands in GaAs at the Γ-point split, due to spin-orbit interaction, into four $j=3/2$ states belonging to the Γ_8 representation, and two $j=1/2$states belonging to the Γ_7 representation. These two are separated from the Γ_8 states by the spin-orbit energy Δ, which is 340 meV in GaAs.[17] We adopt the notation $|j,m_j\rangle$ to represent the Γ_8 and the Γ_7 states, making use of the fact that these states are also eigenstates of the total angular momentum operator $\mathbf{J}=\mathbf{L}+\vec{s}$, with eigenvalue j, and simultaneously eigenstates of its z component, J_z, corresponding to the eigenvalue m_j. Notice that the $\Gamma_8$states $|v1\rangle$ and $|v2\rangle$ both having $j=3/2$ but with $m_j=3/2$ and $m_j=-3/2$, respectively, are called heavy holes states, having their spins well defined, being "up", i.e., aligned with $\mathbf{J}$, and "down", antialigned. They can be represented by using as a basis the three p-type states in the directions x,y, and z:[18]

$$|v1\rangle = \left|\frac{3}{2}\frac{3}{2}\right\rangle = \frac{1}{\sqrt{2}}(|x+iy\uparrow\rangle), \tag{4}$$

$$|v2\rangle = \left|\frac{3}{2}\frac{\bar{3}}{2}\right\rangle = \frac{i}{\sqrt{2}}(|x-iy\downarrow\rangle). \tag{5}$$

The other states, the light hole states $|v3\rangle$ and $|v4\rangle$corresponding also to $j=3/2$, but with $m_j=1/2$ and $m_j=1/2$, and the split-off states $|v5\rangle$ and $|v6\rangle$ corresponding to $j=1/2$ with $m_j=1/2$ and $m_j=-1/2$, do not have well-defined spins,

$$|v3\rangle = \left|\frac{3}{2}\frac{1}{2}\right\rangle = \frac{i}{\sqrt{6}}(-2|z\uparrow\rangle+|x+iy\downarrow\rangle), \tag{6}$$

$$|v4\rangle = \left|\frac{3}{2}\frac{\bar{1}}{2}\right\rangle = \frac{1}{\sqrt{6}}(-|x-iy\uparrow\rangle+2|z\downarrow\rangle), \tag{7}$$

$$|v5\rangle = \left|\frac{1}{2}\frac{1}{2}\right\rangle = \frac{1}{\sqrt{3}}(|z\uparrow\rangle + |x+iy\downarrow\rangle), \tag{8}$$

$$|v6\rangle = \left|\frac{1}{2}\frac{\bar{1}}{2}\right\rangle = \frac{i}{\sqrt{3}}(-|x-iy\uparrow\rangle + |z\downarrow\rangle). \tag{9}$$

The kinetic, Hartree, and the exchange-correlation terms appear in this formalism as the well-known components of the LK matrix.[4] In multilayers and superlattices the mismatches of the valence and conduction bands, which play the roles of confining potentials, are to be added. Differences on the lattice parameters introduce the additional terms of the strain. Here we must also introduce the magnetic potential given by Eq. (3). Two distinct cases may be considered, since a break in the T_d symmetry occurs: magnetization "in-plane" (occurring parallel to the interfaces) $\mathbf{M}_{\|}=M_x\hat{i}+M_y\hat{j}$, and "perpendicular to the plane," $\mathbf{M}_{\perp}=M_z\hat{k}$. The latter is assumed to be in the growth direction, here considered as the z-axis. Notice that in the presence of a confining potential created by the interfaces, $V_c(z)$, the operators $\hat{J}_x$ and $\hat{J}_y$ no longer commute with the LK Hamiltonian. In bulk, however, within the homogeneous magnetization approach, there is no distinction between these two cases. Since we are not trying to explain the origin of the ferromagnetic order in these systems, the occurrence of the magnetization being "in plane" or "perpendicular-to-the-plane" is assumed to be provided by an external weak magnetic field, which does not interfere on the electronic structure, directly.

For the sake of obtaining the LK matrix for heterostructures, it is necessary to calculate first the matrix elements $\langle j,m|V_{\mathrm{mag}}|j',m'\rangle$ for each constituent DMS layer, in bulk. This is easily done by observing that

$$\mathbf{M}_{\perp}\cdot\vec{\sigma}|\uparrow\rangle = M_z|\uparrow\rangle, \tag{10}$$

$$\mathbf{M}_{\perp}\cdot\vec{\sigma}|\downarrow\rangle = -M_z|\downarrow\rangle, \tag{11}$$

and

$$\mathbf{M}_{\|}\cdot\vec{\sigma}|\uparrow\rangle = (M_x+iM_y)|\downarrow\rangle \equiv M_+|\downarrow\rangle, \tag{12}$$

$$\mathbf{M}_{\|}\cdot\vec{\sigma}|\downarrow\rangle = (M_x+iM_y)|\uparrow\rangle \equiv M_-|\uparrow\rangle. \tag{13}$$

Making use of the approximation given in Eq. (3) and the results in Eqs. (10)–(13), we have for the LK matrix of V_{mag} at the Γ point,

$$\tilde{V}_{\mathrm{mag}} = -\frac{x}{6}N_0\beta\begin{pmatrix} 3M_z & 0 & i\sqrt{3}M_- & 0 & \sqrt{6}M_- & 0 \\ 0 & -3M_z & 0 & -i\sqrt{3}M_+ & 0 & -\sqrt{6}M_+ \\ -i\sqrt{3}M_+ & 0 & M_z & 2iM_- & 2\sqrt{2}iM_z & -\sqrt{2}M_- \\ 0 & i\sqrt{3}M_- & -2iM_+ & -M_z & \sqrt{2}M_+ & -2\sqrt{2}iM_z \\ \sqrt{6}M_+ & 0 & -2\sqrt{2}iM_z & \sqrt{2}M_- & -M_z & iM_- \\ 0 & -\sqrt{6}M_- & -\sqrt{2}M_+ & 2\sqrt{2}iM_z & -iM_+ & M_z \end{pmatrix}. \tag{14}$$

During the last years the LK model has been adapted to quantum wells and superlattices (SL), as described in Refs. 18–20. We adopt that approach, using a supercell model. This means that we consider a unit cell consisting of the active region plus a thick insulator layer. The number of DMS layers in the unit cell can be varied at will. We assume, then, an infinite SL in the [001] direction. The multiband effective-mass equation (EME) is represented in terms of plane waves with wave vectors $K=(2\pi/a)l$ (l an integer and a the SL period) equal to the reciprocal SL vectors. A detailed description of the method can be found in Ref. 23. The rows and columns of the 6×6 LK Hamiltonian refer to the Bloch-type eigenfunctions $|j,m_j,\vec{k}\rangle$ of the Γ_8 heavy-hole bands, and the Γ_7 spin-orbit-hole band; $\vec{k}$ denotes a vector of the first Brillouin zone. Expanding the EME with respect to plane waves $\langle z|K\rangle$ means representing this equation in terms of the Bloch functions $\langle \mathbf{x}|j,m_j,\vec{k}+K\mathbf{e}_z\rangle$. For a Bloch function $\langle z|E,\vec{k}\rangle$ of the SL corresponding to energy E and wave vector $\vec{k}$, the EME takes the form

$$\sum_{j',m_j,K'}\langle j,m_j,\vec{k},K|T+H_S+V_{\mathrm{het}}+V_C+V_{\mathrm{xc}}+V_{\mathrm{mag}}|j,m_j',\vec{k},K'\rangle \times\langle j',m_j',\vec{k},K'|E,\vec{k}\rangle = E(\vec{k})\langle j,m_j,\vec{k},K|E,\vec{k}\rangle, \tag{15}$$

where T is the unperturbed kinetic energy term generalized for a heterostructure,[21] H_S is the strain energy term originating from the lattice mismatch, V_{het} is the square potential due to the difference between energy gaps, V_{xc} is the exchange-correlation potential, and V_C is the sum of the Hartree potential with the ionized acceptor potential. Finally, V_{mag} is given by Eq. (3), for each material. The Luttinger parameters and the other terms appearing in the secular equation are to be taken for each epitaxial layer of the SL.[22] For instance, in the case of the magnetic interaction we have

$$\langle j,m,\vec{k},K|V_{\mathrm{mag}}|j',m',\vec{k}',K'\rangle = \langle\vec{k},K|\tilde{V}_{\mathrm{mag}}^{jm;j'm'}g(K'-K)|\vec{k}',K'\rangle, \tag{16}$$

where the integral

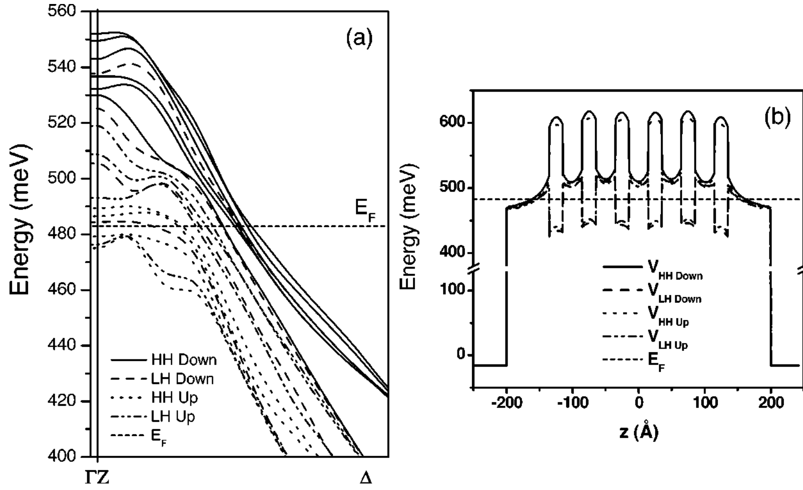

FIG. 2. (a)Valence band structures for GaAs/GaAs:Mn multiple QWs along high symmetry lines Γ-Z and Γ-Δ, with d_1=20 Å and d_2=30 Å. We named the band by its dominant component at the Γ-point. Solid lines correspond to subbands which, at the Γ-point, are mostly heavy holes down, dashed lines to light hole down, dotted lines to heavy hole up, and dotted-dashed lines to light holes up. The Fermi energy is also indicated (short-dashed line). (b) The corresponding potential profile for each carrier, down and up. Energies are reckoned from the top of the Coulomb barrier.

$$g(K'-K) = \frac{1}{d}\int_0^d e^{-iKz} g(z) e^{iK'z} \tag{17}$$

is performed in a DMS layer of width d.

The self-consistent potentials and the charge densities are obtained by solving the multiband EME equation and the Poisson equation,

$$\langle j, m_j, \vec{k}, K | V_C | j', m_j', \vec{k}, K' \rangle = \frac{4\pi e^2}{\kappa} \frac{1}{|K-K'|^2} \times \langle K | \rho^+ + \rho^- | K' \rangle \delta_{j,j'} \delta_{m_j, m_j'}, \tag{18}$$

where κ is the dielectric constant of the host, and ρ^+ and ρ^- are the density of charge of holes andacceptors, respectively, expressed in plane-wave representation.

III. RESULTS

The DMS layers act effectively as barriers or wells for spins parallel (up) and antiparallel (down) to the local average magnetization, depending on the sign of $N_0\beta$ for the valence band, and $N_0\alpha$ for the conduction band. These DMS layers are assumed to be ferromagnetic and metallic, with a 3D equivalent hole density $p = 1\times 10^{20}$ cm^{-3}, a substitutional Mn concentration of 5% at T=0 K, and an average magnetization $\langle M \rangle$=5/2.

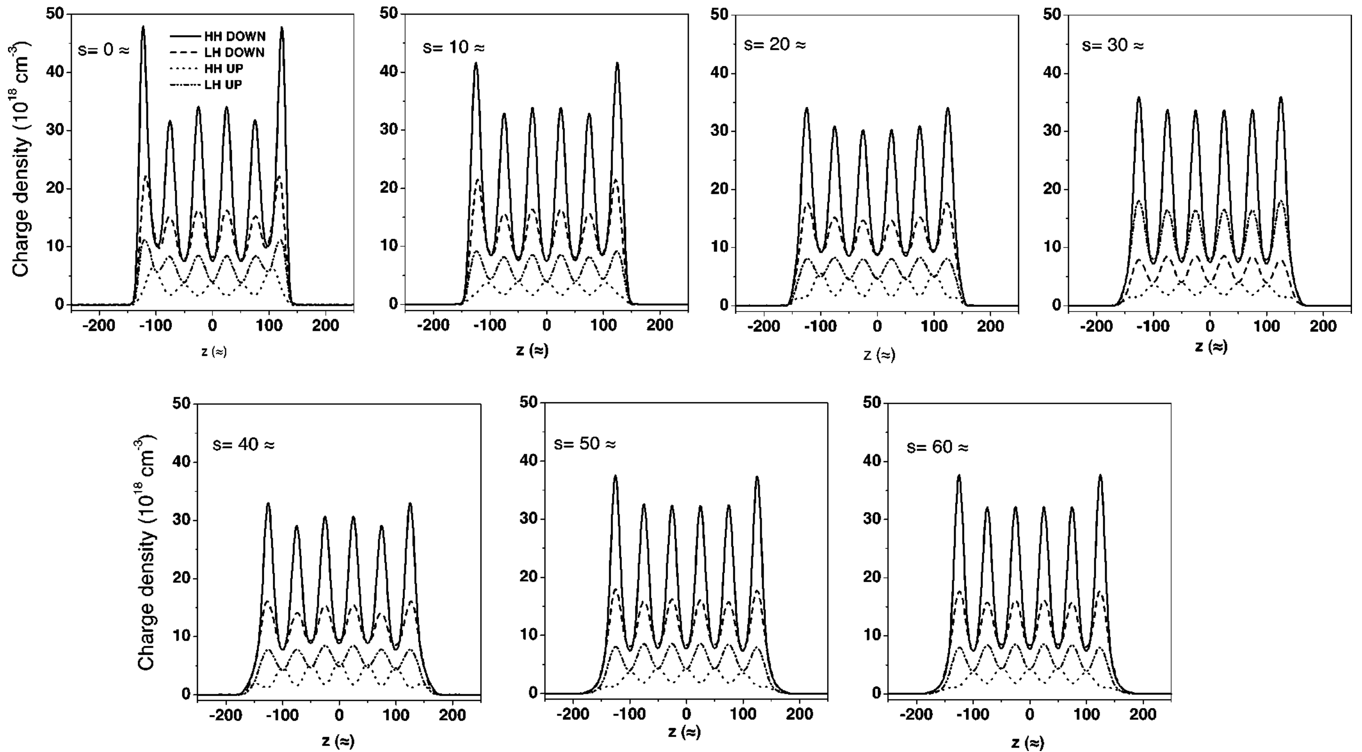

FIG. 3. Density distribution of heavy and light holes for six DMS layers with d_1=20 Å, d_2=30 Å, and lateral GaAs widths s=0,10,20,30,40,50, and 60 Å.

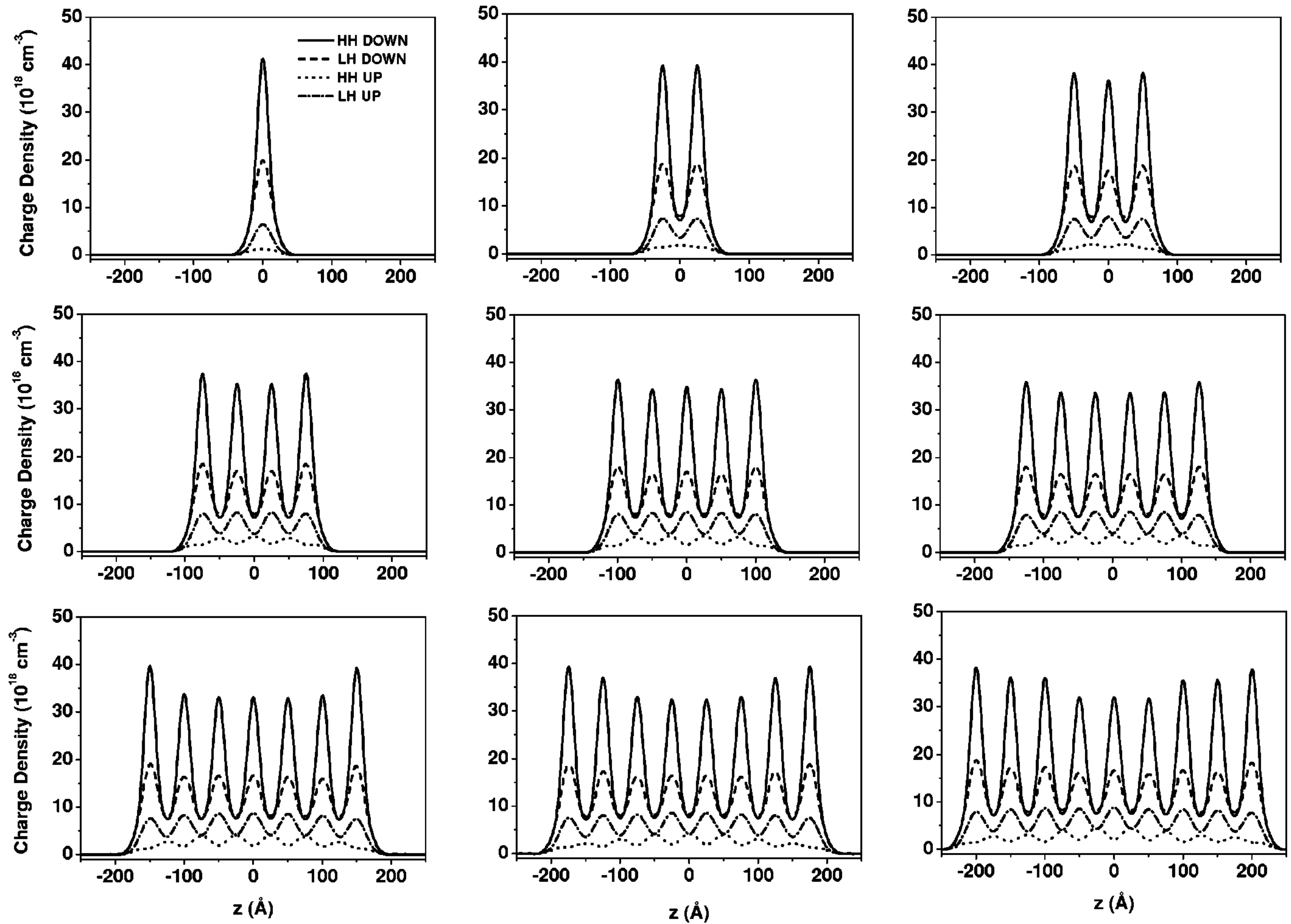

FIG. 4. Particle density of heavy and light holes for a structure consisting from one to nine DMS layers. Widths d_1 and d_2 as in Fig. 1.

In Fig. 2 we present (a) the valence band structure (hole binding energy) and (b) the potential profiles for a system consisting of six DMS layers, with $d_1=20$ Å and $d_2=30$ Å. Energies are reckoned from the top of the Coulomb barrier, as in Ref. 23. The magnetization is assumed to be in the z direction. The subbands are hybrid states, since they are a mixture of all types of holes. However, at the Γ-point the lowest lying states have a dominant hole component. For instance, the first three states are almost entirely "down" heavy holes. The mixing becomes stronger in the higher excited states, and as we go away from the Γ-point. In Fig. 2 we labelled the bands by their dominant component at the Γ-point. Here, "up" and "down" refer to the sign of m_j, the z component of the total angular momentum. In other words, "up" means parallel to the average magnetization, while "down" means antiparallel. The Γ-Δ (Γ-Z) line corresponds to wave vectors $\vec{k}$ perpendicular (parallel) to the SL axis. The Fermi energy is also indicated. Strong nonparabolicity arises in the subbands along the (Γ-Δ) line, which leads to a remarkable anticrossing. We also observe that several levels are occupied, most of them are down heavy and light holes. It is possible to understand this behavior by observing Fig. 2(b), which shows the self-consistent hole band potential profile for each carrier. The confinement for down heavy and light holes are stronger than those for which the z components of the total angular momentum are up.

Figure 3 shows the carrier distributions for the structure with six DMS layers described in Fig. 2. The results are shown for lateral GaAs layers of width $s=0$, 10, 20, 30, 40, 50, and 60 Å. We notice that, except for the heavy hole with $m_j=3/2$ (up), carriers accumulate more in the DMS layers. On the other hand, the up heavy holes tend to concentrate in the nonmagnetic region as a consequence of the strong magnetic repulsion. For $s>50$ Å the carrier distributions become independent of the lateral GaAs widths.

Figure 4 shows the carriers densities for active regions consisting of one to nine DMS layers. We choose $d_1=20$ Å and $d_2=30$ Å. The charge density is plotted for each component. As before, "up" and "down" refer to the sign of the m_j component of the total angular momentum. These results are consistent with the electronic structure shown in Fig. 2, since the lowest levels are mostly down heavy and light holes. Observe that in all multilayered structures (one to nine DMS layers) the charge is concentrated almost entirely within the DMS layers. In contrast, the up heavy hole density is higher in the nonmagnetic regions, for the reasons explained above.

Up to now the distribution of charge in the multilayered structure has been shown in terms of the total angular momentum components of the carriers. For the sake of

FIG. 5. Same as in Fig. 3, for each carrier spin component.

completeness, it is also interesting to know how the charge is distributed in terms of spin polarization. This can be easily obtained, since the light holes are mixed states of up and down spins with defined probabilities. These results are shown in Fig. 5 in terms of the spin components of the charge density. Note that there is a strong spin polarization, dominated by down heavy and light hole spins.

In Fig. 6 we analyze the dependence of the effective two-dimensional hole concentration, N_{2D}, which is the integrated three-dimensional (3D) density along the z direction for each component. The DMS layer widths are varied, while keeping fixed the width of the GaAs layers, $d_2 = 30$ Å. The calculation is performed for six DMS layers. For the down heavy and the light hole, the two-dimensional (2D) densities are much higher than those associated to positive values of m_j. The difference is one order of magnitude in the case of heavy holes, due to their larger effective mass and potential profile discontinuities that provide a higher occupation inside the DMS layers.

Finally, in Fig. 7 we show N_{2D} as a function of the non-magnetic layer width, d_2, with $d_1 = 20$ Å, for each carrier, heavy and light hole (down and up). The calculation is performed for four, five, six, and seven DMS layers.

IV. CONCLUSIONS

In summary, we have investigated the electronic structure of $Ga_{0.95}Mn_{0.05}As/GaAs$ multilayers by using a supercell model in the framework of the Luttinger-Kohn $\mathbf{k} \cdot \mathbf{p}$

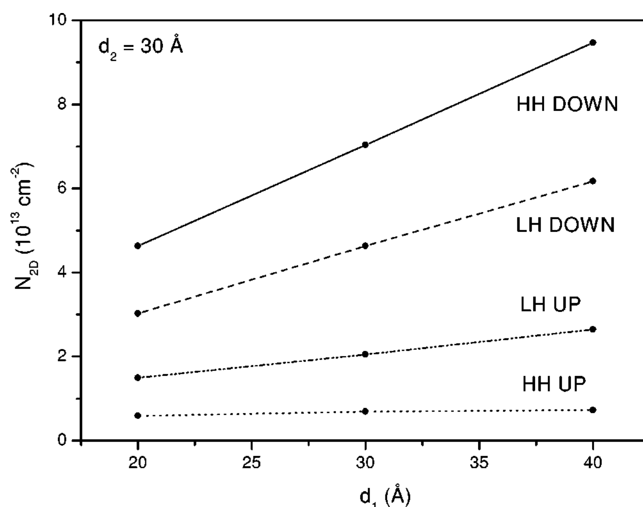

FIG. 6. N_{2D} as a function of the DMS layer width d_1. The width of the nonmagnetic layers are fixed, $d_2 = 30$ Å.

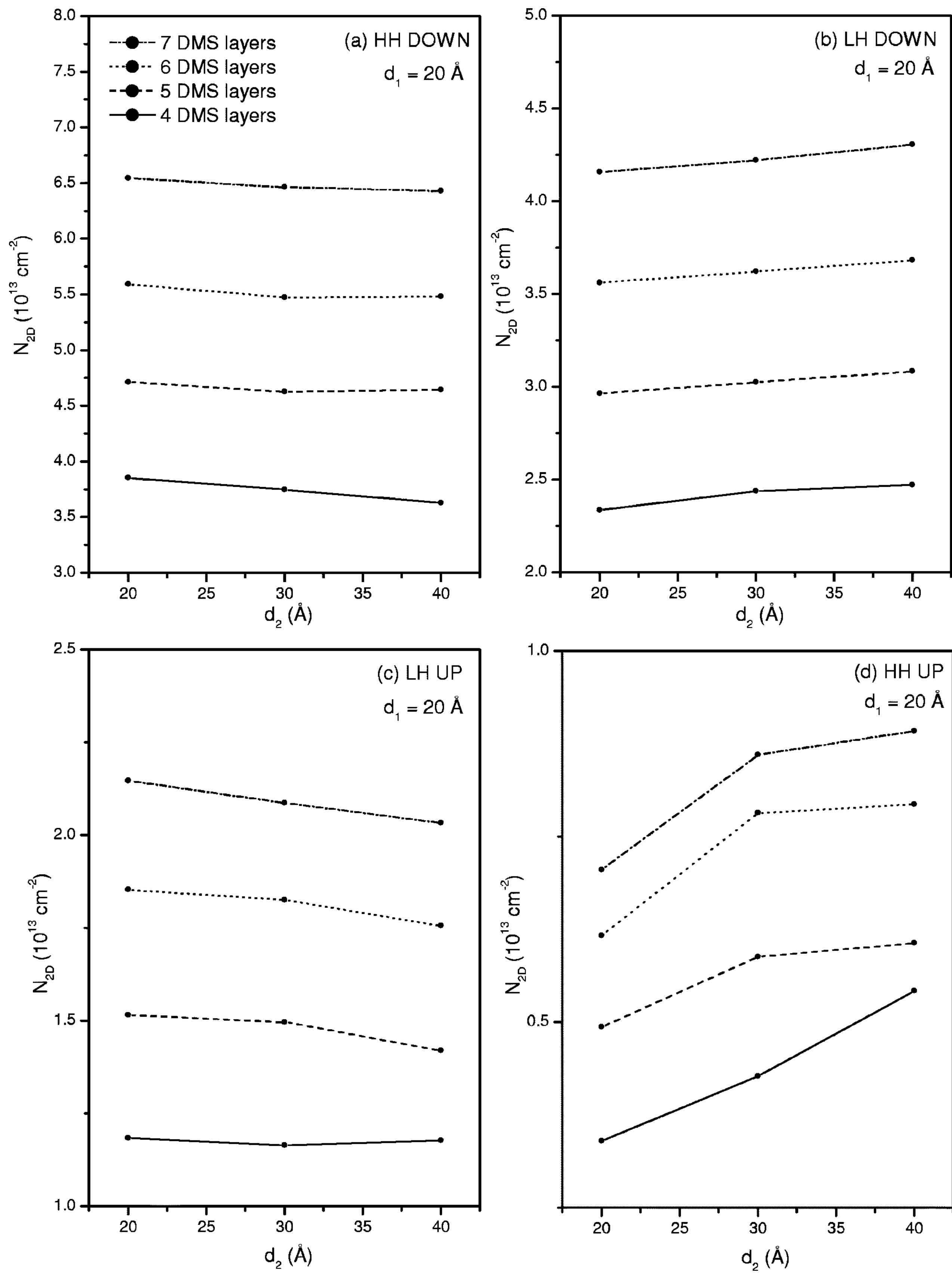

FIG. 7. N_{2D} as a function of the nonmagnetic layer width d_2, for four, five, six, and seven DMS layers. The widths of the DMS layers are fixed, d_1=20 Å.

approximation. The unit in the supercell is a AlAs/n($Ga_{0.95}Mn_{0.05}$As/GaAs)/AlAs structure, with n being the number of DMS layers, grown in the [100] direction. The DMS layers are assumed to be metallic and ferromagnetic at $T=0$ K. A small magnetic field is applied in the growth direction to guarantee the magnetization to be perpendicular to the plane. However it does not affect the electronic structure. Several subbands are occupied. They are mostly heavy holes with $m_j=-3/2$, the carrier density being higher in the DMS layers. However, a non-negligible part of carriers are light holes with $m_j=-1/2$, also concentrated on the same region as the heavy holes. In fact, what is observed is the appearance of two different channels. One of them, highly concentrated on the DMS layers, has the z component of the total angular momentum aligned with the average magnetization. Another, with opposite orientation, has a distribution more concentrated in the nonmagnetic layers of the active region, this latter channel being much less dense. These results are in qualitative agreement with those obtained in Ref. 24 showing the electronic structure calculations in digital ferromagnetic heterostructures of GaAs/(Ga,Mn)As/ and AlAs/(Ga,Mn)As/GaAs using density-functional theory in the local spin-density approximation. As a consequence of both magnetic and Coulomb interactions—here including the hole-hole interaction—the spin-polarized charge tends to be slightly nonperiodically distributed as the number of DMS layers increases. Carriers polarized antiparallel to the magnetization tend to concentrate a little more at the borders of the structure, while carriers polarized in the opposite direction tend to concentrate in the middle.

From the point of view of having a high ferromagnetic transition temperature (recall that we have assumed in our calculation $T=0$ K), it is interesting to have a strong "spin-polarized" charge density in the DMS layers, while keeping some charge in between to guarantee the interlayer interaction.[25,26] However, in order to obtain a high mobility spin-polarized current, a structure should be grown in which the in-plane transport is realized-with spin-polarized carriers concentrated in a region of high mobility, away from the scatterers. Therefore, the ideal distributions of charge and spin depend on the purpose of the structure. The results we have obtained point to the possibility of engineering the spin-polarized charge distribution by the right choice of the magnetic layers and the band mismatches with the nonmagnetic spacers.

ACKNOWLEDGMENTS

This work was supported by CNPq (NanoSemiMat network), and FAPESP. I.C.C.L. thanks the LNMS group for its generous hospitality.

---

*Deceased.

†On leave from Instituto de Física, Universidade do Estado do Rio de Janeiro, Rio de Janeiro, R.J., Brazil.

‡Present address: Departamento de Física,Universidade do Federal de Ouro Preto, Campus Universitrio Morro do Cruzeiro, 35400-000 Ouro Preto, M.G., Brazil.

[1] Y. Ohno, D. K. Young, B. Beschoten, F. Matsukura, H. Ohno, and D. D. Awschalom, Nature (London) **420**, 790 (1999); T. Dietl, H. Ohno, F. Matsukura, J. Cibert, and D. Ferrand, Science **287**, 1019 (2000); T. Dietl, H. Ohno, F. Matsukura, J. Cibert, and D. Ferrand, see also the special issue of Semicond. Sci. Technol. **17** (2002).

[2] F. Matsukura, H. Ohno, A. Shen, and Y. Sugawara, Phys. Rev. B **57**, R2037 (1998).

[3] D. Chiba, K. Takamura, F. Matsukura, and H. Ohno, Appl. Phys. Lett. **82**, 3020 (2003).

[4] J. M. Luttinger and W. Kohn, Phys. Rev. **97**, 869 (1955).

[5] T. Dietl, H. Ohno, and F. Matsukura, Phys. Rev. B **63**, 195205 (2001); T. Dietl *et al.*, Physica E (Amsterdam) **7**, 967 (2000).

[6] B. Lee, T. Jungwirth, and A. H. MacDonald, Phys. Rev. B **61**, 15 606 (2000).

[7] I. Vurgaftman and J. R. Meyer, Phys. Rev. B **64**, 245207 (2001).

[8] M. Abolfath, T. Jungwirth, and A. H. MacDonald, Physica E (Amsterdam) **10**, 161 (2001).

[9] J. Fernández-Rossier and L. J. Sham, Phys. Rev. B **64**, 235323 (2001).

[10] T. Dietl, Semicond. Sci. Technol. **17**, 377 (2002).

[11] H. J. Kim, K. S. Yi, N. M. Kim, S. J. Lee, and J. J. Quinn, Physica E (Amsterdam) **12**, 383 (2002).

[12] J. Jungwirth, B. H. Lee, and A. H. MacDonald, Physica E (Amsterdam) **10**, 153 (2001).

[13] J. Schliemann, J. König, and A. H. MacDonald, Phys. Rev. B **64**, 165201 (2001).

[14] L. Loureiro da Silva, M. A. Boselli, I. C. da Cunha Lima, X. F. Wang, and A. Ghazali, Appl. Phys. Lett. **79**, 3305 (2001).

[15] J. Okabayashi, A. Kimura, O. Rader, T. Mizokawa, A. Fujimori, T. Hayashi, and M. Tanaka, Phys. Rev. B **58**, R4211 (1998).

[16] J. Szczytko, W. Mac, A. Twardowski, F. Matsukura, and H. Ohno, Phys. Rev. B **59**, 12 935 (1999).

[17] J. Wu, H. Yaguchi, K. Onabe, and Y. Shiraki, J. Cryst. Growth **197**, 73 (1999).

[18] See, for instance, R. Enderlein and N. J. Horing, *Fundamentals of Semiconductor Physics and Devices* (World Scientific, Singapore, 1997).

[19] R. Enderlein, G. M. Sipahi, L. M. R. Scolfaro, and J. R. Leite, Phys. Rev. Lett. **79**, 3712 (1997).

[20] S. C. P. Rodrigues, G. M. Sipahi, L. M. R. Scolfaro, and J. R. Leite, J. Phys.: Condens. Matter **13**, 3381 (2001).

[21] S. C. P. Rodrigues, G. M. Sipahi, L. M. R. Scolfaro, and J. R. Leite, Appl. Phys. Lett. **76**, 1015 (2000).

[22] T. P. Pearsall, *Strained-Layer Superlattices: Physics, Semiconductor and Semimetals* (Academic, New York, 1990), Vol. 32.

[23] S. C. P. Rodrigues, G. M. Sipahi, L. M. Scolfaro, and J. R. Leite, J. Phys.: Condens. Matter **14**, 5813 (2002).

[24] S. Sanvito, Phys. Rev. B **68**, 054425 (2003).

[25] M. A. Boselli, I. C. da Cunha Lima, and A. Ghazali, Phys. Rev. B **68**, 085319 (2003).

[26] M. A. Boselli, I. C. da Cunha Lima, A. Troper, J. R. Leite, and A. Ghazali, Appl. Phys. Lett. **84**, 1138 (2004).